

# BLANK-HOLDER FORCE OPTIMIZATION FOR IMPROVING THE STABILITY OF DEEP DRAWING

Ivelin V. IVANOV\*, Svetlana PASKALEVA\*\*

\*University of Rousse, Bulgaria

\*\* Technical University of Varna, branch in Dobrich, Bulgaria

**Abstract.** The explicit finite element method is utilized to simulate the sheet-metal deep drawing process of a flanged cup. The problem is time scaled for more computational efficiency of the simulation. The results of the simulation are compared with experimental results as well as with the results of another implicit finite element simulation for validation. A lot of explicit finite element simulations are used to determine the technological window for the blank holder force and the blank thickness. Investigating the range of blank thickness deviation, it appears to be good choice for objective function corresponding to the process stability. An optimization problem is formulated for searching a stable and reliable forming process with constraints for wrinkling and fracture. The optimal solution is found with high efficiency by an automated computer procedure.

**Keywords:** deep drawing; explicit finite element method; optimization; stability of manufacturing processes

## 1. Introduction

Nowadays, the computer simulations of sheet-metal forming are vastly used in the industry in order to design the product parts, the forming tools, and the parameters of the deep drawing process. The computer simulations are cost efficient and preferable than the experimental trials. Still the computer simulations based on the Finite Element (FE) method are time consuming despite of the computer achievements, when large scale and reliable simulations are in pursuit. Thus the design of the technological process is based on several simulations determining some limiting cases and some acceptable values of the process parameters. The optimization consists of choosing one acceptable set of parameters based on how far is this case from the limiting cases and on the intuition of the decision maker.

The conditions and therefore the parameters of the deep drawing process, however, fluctuate in the manufacturing. The high sensitivity of the process to some parameters or their combinations could cause unwanted results as wrinkling, necking, and cracking or even rupture of the workpiece if the parameters of the deep drawing process are not carefully chosen [1].

The quality of the obtained product is very difficult to be quantified and therefore an optimization problem is difficult to be defined [2]. The sensitivity of the deep drawing process to all factors as material properties, lubrication, temperature, blank position and dimensions, and tool wear should be investigated in order to find the parameters of a robust process, which is very difficult task.

The deep drawing process is comparatively slow and the dynamic forces are negligible. The process could be simulated as quasi-static but it is highly materially nonlinear because of the large plastic strain which appears in the blank during the drawing. The other nonlinearity that appears is the wrinkling of the flange area, which indication is an aim of the simulations. The wrinkling is a result of the local buckling, which is local structural collapse.

The high nonlinearity, however, requires a number of simultaneous linear algebraic equations to be solved many times in the implicit quasi-static FE method [3]. The explicit dynamic FE method is computationally more efficient since there are no simultaneous equations to be solved, but the problem time step of the method is very small for stability and a large number of time steps are necessary to simulate a slow dynamic process [3]. The choice of computationally efficient and less time consuming simulation method gives the opportunity to carry out more simulations and to investigate the deep drawing process better even to solve an automated optimization problem.

## 2. Finite element simulations

FE simulations are based on the time integration of the basic equation of dynamics, which is written in matrix form because of the semi-discretization of the space:

$$\mathbf{M} \cdot \ddot{\mathbf{d}} + \mathbf{K}(\mathbf{d}) \cdot \mathbf{d}(t) = \mathbf{f}(t), \quad (1)$$

where  $\mathbf{M}$  is the mass matrix;  $\mathbf{K}$  is the stiffness nonlinear matrix of the system;  $\mathbf{d}$  is the vector of the nodal displacements and  $\mathbf{f}$  is the vector of the external nodal forces, both depending on the time  $t$ .

The explicit time integration of Eq. (1) requires the internal forces  $\mathbf{q}_n = \mathbf{K}(\mathbf{d}_n) \cdot \mathbf{d}(n)$  to be evaluated for a given displacements  $\mathbf{d}_n$  at time step  $n$ . Then the obtained equation

$$\mathbf{M} \cdot \mathbf{d}_{n+1} = \mathbf{f}(t_n) - \mathbf{q}_n \quad (2)$$

is easy to be integrated in order to get the next displacement  $\mathbf{d}_{n+1}$ . The internal forces can be efficiently calculated element by element and no global stiffness matrix of the system is necessary. If a lumped mass matrix  $\mathbf{M}$  is used, which means the matrix is diagonal, the time integration of Eq. (2) is node-wise and very efficient. The method is straightforward in capturing the nonlinearity of structure stiffness. The disadvantage of the method is the constrained time step,  $\Delta t$ , for stability of the time integration.

The time step should be less than the critical time step  $\Delta t_{cr} = 2/\omega_{max}$  if central difference integration scheme is used, where  $\omega_{max}$  is the maximum eigen frequency of the linearized system. For linear finite elements, the critical time step could be calculated from the sound speed,  $c$ , for the material and the nodal distance,  $h_{nod}$ ,  $\Delta t_{cr} = \min\{h_{nod}/c\}$  for all elements. The sound speed is determined by  $c = \sqrt{E/\rho}$  from the tangential modulus of elasticity,  $E$ , and mass density of the material,  $\rho$ .

The time step for the explicit FE method is of the order of time for sound wave travel in the material of the structure. Thus the method is very suitable for transient problems as impact, but slow dynamic processes as deep drawing manufacturing processes are too long to be simulated with computational efficiency. When the inertia forces are very small, however, the problem simulation could be speed up to the level when their influence becomes noticeable but still ignorable [4]. This is the way to significantly improve the computational efficiency of the deep drawing simulations by the explicit FE method.

The implicit time integration of Eq. (1) requires the nodal displacements,  $\mathbf{d}$ , to be unknown even for the evaluation of the internal forces  $\mathbf{q}$  and the Eq. (1) becomes a set of nonlinear equations. If the process is very slow and not dynamic the inertia forces,  $\mathbf{g} = \mathbf{M} \cdot \ddot{\mathbf{d}}$ , could be neglected and the quasi-static implicit FE method is a method for solving the nonlinear system of equations:

$$\mathbf{K}(\mathbf{d}) \cdot \mathbf{d}(t) = \mathbf{f}(t). \quad (3)$$

The nonlinear equations could be solved by direct methods: linearizing the equations and solving many times a system of linear algebraic equations.

The implicit FE method can solve the problems more precisely than the explicit FE method can do.

The solution of a large number of linear equations is not computationally efficient and the computational time for the direct nonlinear solvers arises significantly with the size of the problem. Their efficiency strongly depends on the nonlinearity and the dynamics of the problem. The iterative solvers could significantly increase the efficiency of large scale problems, but for optimization the degree of discretization is as low as possible for an adequate simulation.

An example of flanged cup deep drawing, well described in [5], is accepted for optimization by FE simulations. The blank material is steel EN10130 FeP01. The thickness of the blank is  $s_0 = 1$  mm and its diameter is  $d_b = 76$  mm. The diameter of the punch is  $d_p = 39.4$  mm and the diameter of the die is  $d_d = 41.7$  mm. The fillet radii of the punch and die are both  $r_p = r_d = 2$  mm. The Blank Holder (BH) presses the blank with force  $F_{BH} = 18$  kN during the deep drawing process with depth  $h_d = 20$  mm. The thickness distribution of the cup and punch force development are examined experimentally and by a implicit FE simulation using AutoForm commercial software by Colgan and Monaghan [5].

Simulations of the example deep drawing process are carried out by the implicit FE method of the commercial software ANSYS<sup>®</sup> [6] and by the explicit FE method of LS-DYNA [7] under the license of ANSYS. The explicit FE method appears to be more computationally efficient if time scaling of the problem is applied. The problem time is reduced to  $t_{pr} = 1.5$  ms and the duration of the simulation calculations is approximately 1.5 min on PC with AMD Athlon<sup>™</sup> 64 3200+ processor. The simulation duration is totally acceptable and gives the opportunity to investigate the problem with many simulations and even to include them in an automated optimization procedure.

The FE discretization and the dimensions of the parts are given in Figure 1. Because of the axial symmetry, only a quarter of the problem is modelled by shell elements. The material of the BH, punch, and die is rigid whilst the material of blank is elastic-piecewise-plastic [7] with characteristics described in Table 1. The blank material could not be strain-rate dependent, because of the time scaling used.

In order to reduce the vibration excitation in the dynamic FE simulations, the BH force evolution is described by the cycloidal law [4]:

$$F(t) = F_{BH} \left( \frac{t}{t_{cl}} - \frac{1}{2\pi} \cdot \sin \frac{2\pi t}{t_{cl}} \right) \quad (4)$$

for the time interval  $0 \leq t \leq t_{cl}$  needed for clamping the blank by the binder, where time  $t_{cl} = 0.3$  ms.

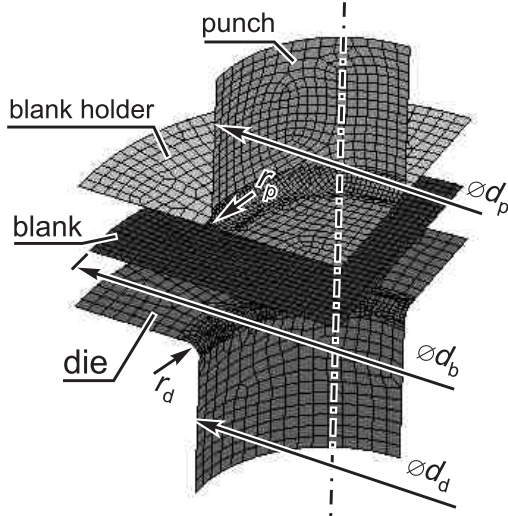


Figure 1. Part discretization

Table 1. Blank material properties

Mass density	Young's modulus	Poisson's ratio						
$\rho = 7.85 \text{ g/cm}^3$	$E = 203 \text{ GPa}$	$\nu = 0.28$						
Yield stress piecewise function of effective plastic strain								
$\tilde{\epsilon}_p, -$	0.0	0.1	0.2	0.3	0.4	0.5	0.6	0.7
$\sigma_y, \text{ MPa}$	230	368	439	496	546	592	634	673

Then the BH force is left constant  $F(t) = F_{BH}$  up to the problem termination time  $t_{pr}$ . The time interval  $t_{cl} < t < t_{dm}$ , where  $t_{dm} = 0.5$  ms, is necessary for damping of the excited vibrations of the blank. The punch starts to travel at time  $t_{dm}$  and its displacement,  $h(t)$ , is described by the cycloidal law [4]:

$$h(t) = h_d \cdot \left[ \frac{t - t_{dm}}{t_{pr} - t_{dm}} - \frac{1}{2\pi} \cdot \sin \frac{2\pi \cdot (t - t_{dm})}{t_{pr} - t_{dm}} \right] \quad (5)$$

for the time interval  $t_{dm} \leq t \leq t_{pr}$ . The diagrams of binder force and punch displacement are given in Figure 2.

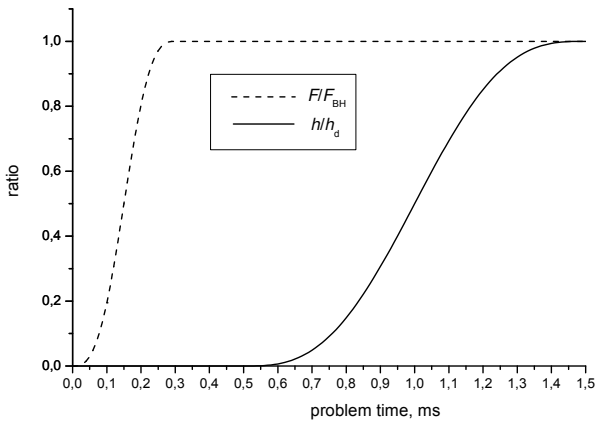


Figure 2. Force and displacement diagrams

The friction between the parts plays a significant role in the deep drawing process. Coulomb's friction is prescribed for the contact between the parts in the FE simulation. There is no value available for the friction coefficient,  $\mu$ , in [5]. In explicit FE simulations, the contact between the blank and the BH and between the blank and the die is not well maintained because of the excited vibrations of the blank. Therefore the friction coefficient in such simulations should be slightly higher than the experimentally determined in order to give the same results.

The most affected parameter by the friction coefficient is the punch force development during the deep drawing. Several values of the friction coefficient,  $\mu$ , are tried out and finally the closest punch force graph to the experimental one is reached for  $\mu = 0.1$ . Comparison between the obtained in the FE simulation punch force and the experimentally determined as well as the obtained in [5] by a FE simulation is given in Figure 3. Good agreement is achieved although the present simulation shows more dynamics in the force development, which pertains to the explicit FE method. The higher punch force in the present simulation is due to the inertia forces which just start to become significant at this degree of the problem time scaling.

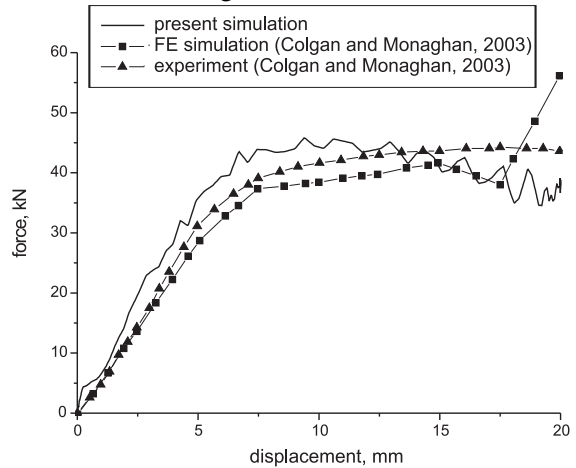


Figure 3. Punch force development

The strain distribution in the cup is the most reliable characteristic which verifies the adequacy of the simulation. The thickness change of the blank is direct result of the strain evolution in the material. The thickness reduction of the blank at the end of the explicit FE simulation is given in Figure 4, pointed on the model of the cup. There is no spring back implicit step at the end of the simulation. Based on inspections of the thickness reduction at

different finite elements, the thickness,  $s$ , at eight points of the cup profile is determined by Colgan and Monaghan in [5].

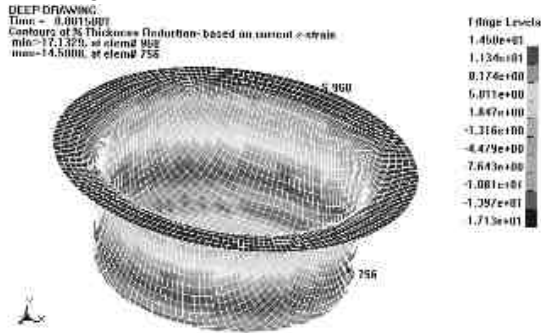


Figure 4. Thickness reduction

The graph of thickness distribution at the points is shown in Figure 5 and the result is compared with the results of the experiment and with the other FE simulation described in [5]. The thickness of the cup at the end of the present simulations is a little bit higher at the wall points and the minimum is closer to the bottom, where the thickness is even lower than in the experiment. This distribution of the thickness in the present simulation is due to the inertia forces added and changing the plastic flowing in the sheet-metal.

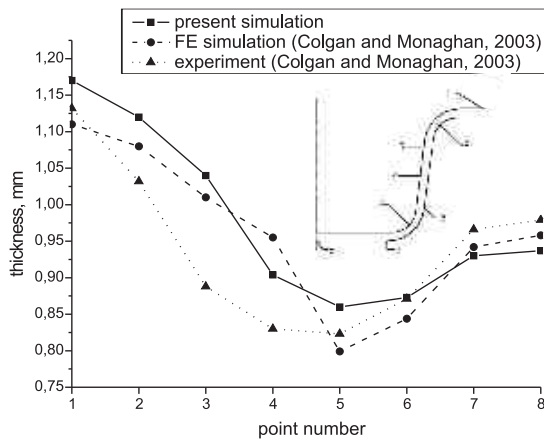


Figure 5. Thickness distribution

The explicit FE method is utilized to simulate adequately the manufacturing process of deep drawing of a cup. Precise results are not in pursuit but the computational efficiency is important. The carried out simulation appears to be enough adequate and efficient in order to be accepted for studying the manufacturing process by FE simulations.

### 3. Determination of the technological window

The BH force is needed to prevent the wrinkling of the flange area of the workpiece,

which is going into local buckling as a result of the compressive hoop stress. The necessary minimal force depends on the material properties and the thickness of the blank for given tools dimensions and drawing depth. The very high BH force could cause necking, cracking, and rupture of the cup. The thickness of the blank should always provide its formability and only in some cases it is constrained by the strength requirements. The choice of the BH force together with the blank thickness is important for the design of the deep drawing manufacturing process. The technological window of those two parameters is determined for the validation example of the previous section by many computer simulations using the explicit FE method.

The local buckling and the resultant wrinkling are naturally obtained in the explicit FE simulations. The method can capture any nonlinearity of the structure behaviour. Since vibrations and shock waves are excited in the dynamic FE methods it is not needed some imperfection or other disturbances to be defined in the model. The wrinkling of the flange area is determined visually by inspection in the postprocessing of the FE simulation. As a result of the wrinkling, the BH is lifted up and the wrinkle heights,  $h_w$ , can be measured by the BH displacement. For more precise decision a limit of the wrinkle heights,  $h_{lim}$ , can be defined. The limit height for this study is accepted to be  $h_{lim} = 0.5 \cdot s_0$  and wrinkling is counted if  $h_w > h_{lim}$ .

The cracking and the rupture of the work-piece can be predicted by suitable failure criterion for the material. Very precise determination of the fracture is not necessary, because the steps of the BH force change in such an investigation are comparatively large. The determination of the fracture by comparison of the strain states in all finite elements with the Forming Limit Curves (FLC) of the material is considered as very complicated and not necessary. The effective plastic strain,  $\tilde{\epsilon}_p$ , is accepted as a failure criterion here. The effective plastic strain is limited to  $\tilde{\epsilon}_{lim} = 0.7$ . If  $\tilde{\epsilon}_p > \tilde{\epsilon}_{lim}$  in some shell element a failure is counted and it is deleted from the model database. The failure in the FE model can be found visually by inspection in the postprocessing of the simulation or by the messages written in the output files.

The technological window is determined by varying the blank thickness,  $s_0$ , and the BH force,  $F_{BH}$ . The values accepted here for this study are as follows:  $s_0 = 0.6, 0.7, 0.8, 0.9,$  and  $1$  mm;  $F_{BH} = 1, 2, 4, 6, 8, 10, 20, 50, 100, 120, 140, 160,$  and  $180$  kN.

In this way, 65 combinations of the investigated parameters are obtained and 65 FE simulations are carried out. The fracture and the wrinkling, which have appeared in the simulations, determine the technological window given by the limiting curves in Figure 6.

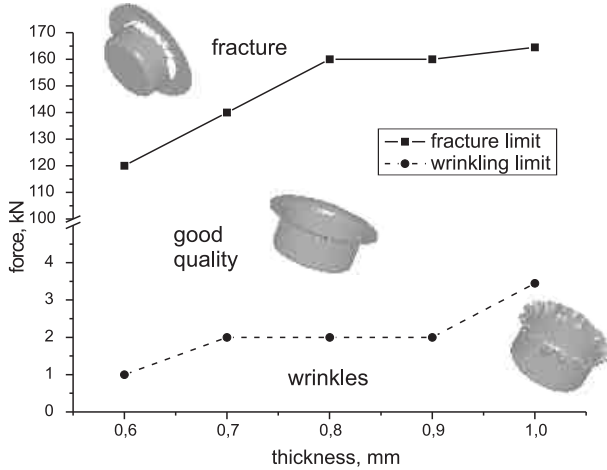


Figure 6. Technological window of BH force and blank thickness

The technological window could tell us what values the BH force should not have but not what the best value of the force is. Any value from 6 kN to 100 kN is acceptable for the BH force when the blank thickness ranging from 0.6 mm to 1 mm. The range is quite large and if a concrete value is chosen there is no guarantee that if the lubrication is missing, for instance, the cup will not be fractured. An optimization problem is necessary to be defined with a proper objective function and the problem solution could give the answer about the best value of the BH force.

#### 4. Optimization for stability

In order to optimize a problem, an objective function is necessary, which arguments are the optimal solution, when its minimum is reached. When the quality of manufacturing is the criterion, the number of defective products for variety of conditions can be the objective function. But, when the quality of a product at the stage of its design is considered as a criterion, the objective function is a Boolean function, which is difficult to be minimized in an optimization procedure. Some authors try to find an appropriate objective function and to quantify the quality criterion.

Schenk and Hillmann [8] have plotted the strain state points of all finite elements in the strain plane of major and minor strains as well as the FLC. The fracture criterion is the sum of distances of all points

in the dangerous area behind the FLC to the limiting curve weighted by the finite element volume. The criterion is zero if the quality is good and no point is in the dangerous area. The criterion is like a penalty function which value increases when unwanted result occurs. The strain in the thickness direction of shell elements is result of the strain state. The constant strain in the thickness direction is plotted as a straight line in the strain plane [8]. The wrinkling criterion is determined by a limiting line corresponding to a constant strain in the thickness direction. It is calculated as a sum of distances of the points in the dangerous area to the line.

Gantar and Kuzman [1] as well as Gantar et al. [2] used similar approach plotting the strain state points on the strain plane. The ratio of the distances to the dangerous point and to the FLC is used as a measurement of the danger. The maximum of two [1] or six [2] dangers gives the real number value of the objective function. Ohata et al. [9]; Ohata et al. [10] used mean square deviation of the workpiece thickness as objective function in the optimization of the deep drawing process. The uniform thickness seems to be a quality requirement.

The blank thickness change is a reflection of both quality dangers in the deep drawing process. If the thickness decreases somewhere in the workpiece, the danger of fracture is going high. The risk of wrinkling becomes higher if the thickness of the blank increases at the flange area. The objective function defined here is the range of the thickness deviation,  $\delta$ , which can be evaluated from the strain in the thickness direction of the blank,  $\epsilon_n$ , where  $n$  denotes the normal of the shell elements.

For each shell finite element with reduced integration, the strain in the thickness direction is calculated at the "top" surface,  $\epsilon_{ntop}$ , and at the "bottom" surface,  $\epsilon_{nbot}$ . The average strain in the thickness direction:

$$\bar{\epsilon}_n = \frac{\epsilon_{ntop} + \epsilon_{nbot}}{2} \quad (6)$$

is taken as a thickness change measurement of the shell element. The objective function is defined as the range of the average strain in the thickness direction for all elements of the blank FE model:

$$\delta = \max \bar{\epsilon}_n - \min \bar{\epsilon}_n. \quad (7)$$

The range of the thickness deviation,  $\delta$ , is considered more sensitive to the defective situations in the deep drawing than the mean square deviation [9, 10], which smear the reasons of the defects.

In order to examine the behaviour of the objective function, its values are calculated for all FE simulations that have been carried out for the

determination of the technological window in the previous section. The simulations ended with defective products should be excluded from the consideration. The obtained values of the objective function,  $\delta$ , are only 30 in the rectangle area of  $F_{BH} \in [6, 100]$  kN and  $s_0 \in [0.6, 1.0]$  mm. Since the number of the points is very small and they are distributed unevenly in the rectangle, an interpolation of the thickness deviation range,  $\delta$ , using cubic polynomials in MATLAB [11] software environment is applied. The contour plot of the smoothed objective function,  $\delta$ , is shown in Figure 7.

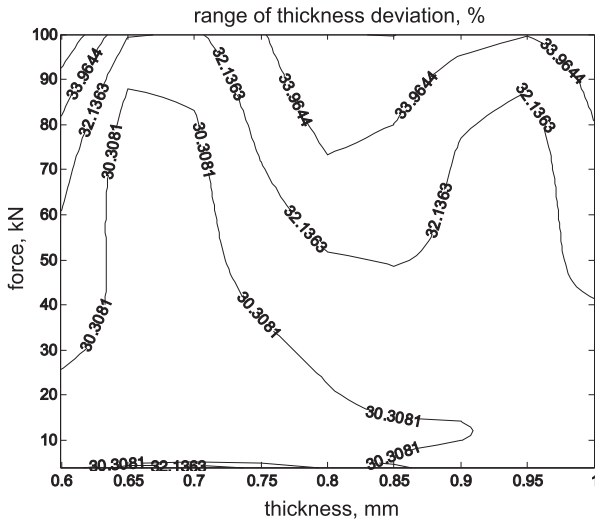


Figure 7. Distribution of the blank thickness deviation range

The plot shows that the objective function increases rapidly when the point is approaching the wrinkling limit curve. It increases when the other limit curve is being approached, too. Those characteristics of the function show that it is suitable for objective function determining the stability of the deep drawing process. The optimal solution should be expected to be closer to the wrinkling limit than to the fracture limit in the technological window. This conclusion coincides with the results obtained by Gantar et al. [2].

The blank thickness deviation range is chosen for objective function and together with parameters range constraints and constraints for fracture and wrinkling the formulation of the optimization problem is as follows:

$$\min_{(F_{BH}, s_0)} \delta = \delta(F_{BH}, s_0), \quad (\%) \quad (8)$$

$$\text{s.t.} \quad 0.05 \leq F_{BH} \leq 20, \quad (\times 10 \text{ kN}) \quad (9)$$

$$0.3 \leq s_0 \leq 1.6, \quad (\text{mm}) \quad (10)$$

$$N_{fe} - 0.5 \leq 0 \quad (11)$$

$$h_w - h_{lim} \leq 0, \quad (\text{mm}) \quad (12)$$

where  $N_{fe}$  is the number of the reported shell-element failures during the FE simulation. The measurement units are chosen to give high and equal sensitivity of the objective function,  $\delta$ , to its arguments,  $F_{BH}$  and  $s_0$ .

The formulated optimization problem has been solved in MATLAB software environment utilizing the functions of its Optimization Toolbox. Several methods available in the Optimization Toolbox have been applied and the most efficient solution of the problem is obtained by Sequential Quadratic Programming in combination with Line Search. The Hessian matrix is updated at each iteration by BFGS method [11]. The parameter constraints (9) and (10) can be directly formulated, but the constraints (11) and (12) for fracture and wrinkling need to be calculated in separate function. The calculation of this function leads to additional FE simulations for applying the constraints without objective function calculation. In order to avoid multiple FE simulations, some of them for objective function calculations and others for constraint calculations, and to make the code more efficient a new objective function,  $f$ , is formulated, which includes the constraints (11) and (12) as a penalty. The reformulated optimization problem is as follows:

$$\min_{(F_{BH}, s_0)} f = \delta + N_{fe}^2 + h_w^3 \quad (13)$$

$$\text{s.t.} \quad 0.05 \leq F_{BH} \leq 20, \quad (\times 10 \text{ kN})$$

$$0.3 \leq s_0 \leq 1.6, \quad (\text{mm}).$$

The optimization iterations begin from a starting point and try to find a local minimum of the function,  $f$ .

The results of nine local searches from different starting points are given in Table 2. The global optimal solution is obtained at BH force  $F_{BH} = 6.1$  kN and blank thickness  $s_0 = 0.3$  mm, which is the lower boundary of the thickness (the underlined values). The thickness deviation range is  $\delta = 26.54$  %, which should provide better formability of the cup and therefore more stability of the deep drawing process.

The local minimum is reached at the range limit of the thickness 0.3 mm in eight cases of different starting points, but in one case the local minimum is reached at different blank thickness of 0.8 mm (case 7). This shows that the objective function is not very smooth and global optimization technique should be applied. The local minimums are at the blank thickness  $s_0 = 0.3$  mm in the most of the cases but at different BH forces,  $F_{BH}$ , which shows that

the sensitivity of objective function to the BH force is low, at least when the minimum of the function is on its constraint.

Table 2. Global minimum search

No.	Start. point		Number of iters.	FE simuls.	Local minimum		
	$F_{BH}$ kN	$s_0$ , mm			$F_{BH}$ kN	$s_0$ , mm	$\delta$ %
1	20.0	0.5	3	12	1.66	0.30	27.79
2	10.0	0.5	3	13	5.49	0.30	26.55
3	5.0	0.5	2	10	6.41	0.30	26.56
4	40.0	1.0	3	13	4.86	0.30	26.66
5	18.0	1.0	3	12	2.05	0.30	26.73
6	10.0	1.0	4	23	15.73	0.30	27.63
7	60.0	1.3	1	7	54.10	0.80	32.64
8	30.0	1.3	2	10	6.25	0.30	26.57
9	10.0	1.3	3	13	6.09	0.30	26.54
total and global			24	116	6.09	0.30	26.54

In order to investigate the problem better, the lower boundary of the blank thickness constraint (10) is changed and the local minimum of objective function is searched beginning from four different starting points. The optimal results for the different lower boundaries of the blank thickness constraint are given in Table 3. They show that the optimal BH force initially increases when the blank thickness is increasing, but for the high thickness of 1.3 mm, the optimal BH force drops down to 4.14 kN and it is at the edge of the flange wrinkling. The thickness deviation range increases with the increasing of the blank thickness.

Table 3. Optimal force for constrained thickness

$s_0$ , mm	0.30	0.55	0.80	1.05	1.30
$F_{BH}$ , kN	6.09	8.28	14.13	14.98	4.14
$\delta$ , %	26.54	27.68	29.12	31.53	33.37

The time necessary for each local optimization of the problem is approximately 20 min when it runs on PC with AMD Athlon™ 64 3200+ processor. The problem could be solved for different starting points and the path of the optimization iterations can be used to investigate the design space. The solution is automated since the MATLAB optimization script reads the ASCII output files of LS-DYNA and writes the parameters in its ASCII input file to run the programme with it. The solution time is totally acceptable for such investigation of the problem.

## 5. Conclusions

The explicit FE method is successfully utilized to simulate the sheet-metal deep drawing process. The simulations can adequately predict the defects in the product as fracture and wrinkling. The time scaling of the problem is possible because of the slow dynamics of the process and it significantly increases the computational efficiency of the FE simulations. The technological window of the parameters of the manufacturing process can be determined by many FE simulations. Finding appropriate objective function as the blank thickness deviation range, an optimization problem for improving the stability of the deep drawing process can be formulated. The optimization procedure is automated and it gives the solution in acceptable time. The procedure is readily available in the commercial computer software and it is easy to be realized in order to solve deep drawing optimization problems in the industry.

## Acknowledgements

The authors wish to express their gratitude to Prof. Georgi Popov of University of Rouse for his kind support.

## References

- Gantar, G., Kuzman, K.: *Sensitivity and stability evaluation of the deep drawing process*. Journal of Materials Processing Technology, Vol. 125–126 (2002), p. 302–308
- Gantar, G., Kuzman, K., Filipič, B.: *Increasing the stability of the deep drawing process by simulation-based optimization*. Journal of Materials Processing Technology, Vol. 164–165 (2005), p. 1343–1350
- van de Boogaard, A.H., Meinders, T., Huétink, J.: *Efficient implicit finite element analysis of sheet forming processes*. International Journal for Numerical Methods in Engineering, Vol. 56 (2003), p. 1083–1107
- Kutt, L.M., Pifko, A.B., Nardiello, J.A., Papazian, J.M.: *Slow-dynamic finite element simulation of manufacturing processes*. Composite Structures, Vol. 66 (1998), p. 1–17
- Colgan, M., Monaghan, J.: *Deep drawing process: analysis and experiment*. Journal of Materials Processing Technology, Vol. 132 (2003), p. 35–41
- \*\*\*: ANSYS 8.1 (2004) ANSYS Inc., Canonsburg, PA.
- \*\*\*: LS-DYNA 970 (2003) Livermore Software Technol. Corp., Livermore, CA.
- Schenk, O. Hillmann, M.: *Optimal design of metal forming die surfaces with evolution strategies*. Composite Structures, Vol. 82 (2004), p. 1695–1705
- Ohata, T., Nakamura, Y., Katayama, T., Nakamachi, E., Nakano, K.: *Development of optimum process design system by numerical simulation*. Journal of Materials Processing Technology, Vol. 60 (1996), p. 543–548
- Ohata, T., Nakamura, Y., Katayama, T., Nakamachi, E., Omori, N.: *Improvement of optimum process design system by numerical simulation*. Journal of Materials Processing Technology, Vol. 80–81 (1998), p. 635–641
- \*\*\*: MATLAB 6.5 (2002) The MathWorks Inc., Natick, MA.